J. Indones. Math. Soc.
Vol. 32, No. 01 (2026), pp. 1–31.

Cost-Effectiveness and Optimal Control Strategies for Managing Marburg Virus Infections

Zasmin Haque[1,3], Md. Mashih Ibn Yasin Adan[2], and Md. Kamrujjaman[3*]

[1]Department of Mathematics, American International University-Bangladesh, Bangladesh
[2]Department of Mathematics, Kishoreganj University, Bangladesh

[3]Department of Mathematics, University of Dhaka, Bangladesh

Abstract. This study develops a mathematical model to investigate the transmission dynamics of Marburg Virus Disease (MVD), integrating two time-dependent control strategies, primarily focusing on isolating infected individuals. Optimal control strategies are designed using Pontryagin's Maximum Principle to minimize the spread of the infection. The basic reproduction number is calculated to identify the disease-free and endemic equilibrium points. The analysis highlights the effectiveness of interventions such as personal protective measures (e.g., wearing masks, maintaining hand hygiene, and avoiding risky dietary practices) combined with supportive hospital therapy in curbing disease transmission. Model simulations validate the impact of these optimal control strategies, while a cost-effectiveness analysis identifies the most efficient approach for disease management. Additionally, the study examines how individuals with robust immune systems can influence the overall dynamics of Marburg virus transmission.

Key words and Phrases: Optimal control, cost-effectiveness, natural immunity, numerical simulation, protective measure.

1. Introduction

Marburg disease is a rare but severe hemorrhagic fever caused by the Marburg virus, a member of the Filoviridae family. This disease can lead to serious illness and has a high fatality rate, with case fatality rates varying from 24% to 88% depending on the virus strain and case management [1, 2]. The virus was first identified in 1967 in West Germany and is transmitted through direct contact with infected individuals or animals, not through the air. Symptoms include sustained high fevers, confusion, irritability, and, in advanced stages, orchitis [3]. Since its

*Corresponding author : kamrujjaman@du.ac.bd
2020 Mathematics Subject Classification: 92D30, 49J15, 34C60, 91B06.
Received: 24-11-2024, accepted: 05-12-2025.

emergence, Marburg virus outbreaks have been reported in several countries, including Angola, Kenya, and Uganda, with a recent outbreak in Ghana in June 2022 [2]. These incidents highlight the ongoing risk of transmission, particularly through unprotected contact in healthcare settings and communities. The disease's impact varies significantly across regions. For instance, Uganda reported a total of 19 cases from 2012 to 2017, resulting in a mortality rate of 42%. Angola recorded the highest number of cases in 2005, with 374 cases and a mortality rate of 88%. The Democratic Republic of the Congo documented 154 cases between 1998 and 2000, exhibiting an 83% mortality rate. In contrast, both the United States and Yugoslavia showed significantly lower case counts and fatalities, with mortality rates of 0% [2]. This variability underscores the importance of context in understanding the disease's epidemiology. This study employs a mathematical model to investigate the transmission dynamics of Marburg virus disease (MVD), focusing on two time-dependent control strategies that prioritize the isolation of infected individuals. Utilizing optimal control strategies based on Pontryagin's Maximum Principle [4, 5], we calculate the basic reproduction number (R_B) to identify disease-free and endemic equilibrium points. Our findings indicate that effective control measures, including isolation of infected individuals and personal protective practices, can significantly reduce disease transmission. Additionally, we explore the role of robust immune systems in influencing infection dynamics, providing valuable insights for effective MVD management and highlighting the importance of both individual behaviors and broader healthcare strategies in combating infectious diseases.

In this study, we constructed a deterministic mathematical model to analyze the transmission dynamics of Marburg Virus Disease (MVD). The model incorporates two time-dependent control strategies, primarily focusing on the isolation of infected individuals. By employing Pontryagin's Maximum Principle [6, 7, 8], we determined optimal control strategies that minimize infection levels [9]. The main goal of our research is to explore how isolating infected individuals affects the spread of MVD [10, 11]. We assessed the influence of individuals with natural immunity and the importance of supportive hospital care in controlling the overall infection rate. To achieve this, we calculated the basic reproduction number (R_B), a crucial epidemiological metric representing the average number of secondary infections generated by a single infected individual in a fully susceptible population. This calculation helps identify both disease-free and endemic equilibrium points [12, 13], providing insights into the conditions required for disease eradication or persistence. Our model also accounts for personal protective measures, such as wearing masks and practicing good hygiene, which are vital for managing infection spread. Furthermore, we explored complementary and alternative medicine (CAM) practices, including herbal remedies and nutritional support, as adjuncts to conventional care [14, 15]. While these treatments can improve health and well-being, they should be used under the guidance of qualified practitioners to ensure safety and effectiveness. Simulations of the optimal control model consistently demonstrate a significant reduction in infection levels when these strategies are applied [16, 17]. This highlights the importance of a multifaceted approach to combating

MVD, where isolation, natural immunity [18], personal protective measures, and supportive medical care work together to mitigate disease impact. Maintaining a healthy diet is crucial for a strong immune system, which is essential for eradicating viral infections [19, 20]. Key recommendations include:

- Incorporating a diverse selection of fruits and vegetables rich in essential vitamins, minerals, and antioxidants.
- Including lean protein sources such as poultry, fish, beans, and legumes to support tissue repair and growth.
- Consuming healthy fats from avocados, nuts, seeds, and olive oil.
- Incorporating probiotics through yogurt and fermented foods to maintain gut health.
- Staying hydrated and engaging in regular physical activity.

Additionally, adequate sleep, stress management techniques (such as meditation and yoga), and good hygiene practices are vital for overall health. Avoiding smoking and limiting alcohol intake further enhance immune function. Spending time outdoors for sunlight exposure helps produce vitamin D, crucial for immune health. Numerous herbal formulations have demonstrated effectiveness in treating viral infections [21, 22]. Herbal supplements like echinacea, elderberry, and garlic are believed to enhance immunity. Maintaining a healthy weight, fostering social connections, and engaging in regular exercise contribute to overall health and improved immune responses. This study offers valuable insights into the effective management of Marburg Virus Disease, emphasizing the significance of individual actions in strengthening the immune system and the role of systemic healthcare strategies in controlling infectious diseases.

2. Model Formulation

Mathematical modeling provides representations of real-world situations, enabling predictions and insights into viral diseases [23, 24, 25]. In this study, we develop a deterministic SEIR (Susceptible, Exposed, Infected, Recovered) model that incorporates control strategies [26]. The total human population $N_H(t)$ at any time t is divided into five groups: $S(t)$ for susceptible individuals, $E(t)$ for exposed individuals, $I_{so}(t)$ for isolated individuals (either asymptomatic or symptomatic), $I_{nf}(t)$ for currently infected individuals, and $R(t)$ for recovered individuals. The total population is expressed as:

$$N_H(t) = S(t) + E(t) + I_{so}(t) + I_{nf}(t) + R(t). \tag{2.1}$$

The model can be explained as follows,

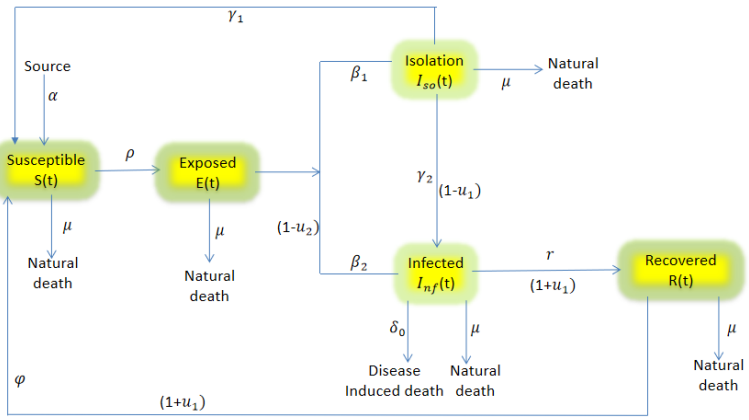

FIGURE 1. SEIR compartmental model of MVD.

All parameters in the model are positive. The parameter α represents the source rate of the human population, while ρ denotes the force of infection affecting exposed individuals. The number of exposed individuals can become infected through asymptomatic individuals in isolation and symptomatic individuals at rates β_1 and β_2, respectively. The recovery rate for those infected with Marburg Virus Disease (MVD) is denoted by r. To enhance the realism of our model, we incorporate optimal control interventions that respond to infection levels and disease management. Thus, we introduce time-variant control functions aimed at minimizing infection rates, which are crucial for addressing infectious disease challenges [9, 12]. The control functions are defined as follows:

- $u_1(t)$: Control against infections transmitted from isolated and infected individuals.
- $u_2(t)$: Control aimed at MVD prevention efforts.

The assumptions regarding the differential equations of our model can be outlined as follows:

$$\begin{cases} \frac{dS(t)}{dt} &= \alpha + \gamma_1 I_{so} + \varphi R(1+u_1) - \rho SE - \mu S \\ \frac{dE(t)}{dt} &= \rho SE - \beta_1 E - \beta_2 E(1-u_2) - \mu E \\ \frac{dI_{so}(t)}{dt} &= \beta_1 E - \gamma_1 I_{so} - \gamma_2 I_{so}(1-u_1) - \mu I_{so} \\ \frac{dI_{nf}(t)}{dt} &= \beta_2 E(1-u_2) + \gamma_2 I_{so}(1-u_1) - r I_{nf}(1+u_1) - (\mu+\delta_0) I_{nf} \\ \frac{dR(t)}{dt} &= r I_{nf}(1+u_1) - \varphi R(1+u_1) - \mu R \end{cases} \tag{2.2}$$

with the initial conditions given by $S(0) \geq 0, E(0) \geq 0, I_{so} \geq 0, I_{nf} \geq 0, R(0) \geq 0$. The following Table 1 shows the values of the parameters.

TABLE 1. Description and estimation of parameters.

Notation	Descriptions	Quantities	Measurements	Citations
α	Birth rate of susceptible individuals	$0.025 - 0.25$	day^{-1}	Estimated
ρ	Rate of exposure for individuals	0.152	day^{-1}	Fitted
β_1	Rate of isolation for individuals	$0.0138 - 0.139$	Dimensionless	Fitted
β_2	The infection rate of exposed population	0.013	Dimensionless	Fitted
φ	Reintegration rate of recovered individuals to susceptible individuals	0.004	day^{-1}	Estimated
γ_1	The rejoining rate of isolation individuals to susceptible individuals	0.127	day^{-1}	Estimated
γ_2	The rate at which isolated individuals get infected	0.329	day^{-1}	Estimated
δ_0	Mortality rate due to the disease	0.09	day^{-1}	Estimated
r	Recovery rate of infected individuals	0.4027	day^{-1}	Estimated
μ	Natural mortality rate	$0.075 - 0.78$	day^{-1}	Assumed
u_1	Control parameter, be the efforts aimed at preventing from the disease through personal protective measure; including strong immunity transmitted from isolated individuals	0.9	Dimensionless	Fitted
u_2	The control variable, be the attempt to take medical treatment and also including strong immunity recovered from infected individuals	0.001	Dimensionless	Fitted

The basic reproduction number of (2.2) is defined as follows (refer to Appendix A for detailed derivation):

$$R_B = \frac{\alpha\rho}{\mu\left\{\beta_1 + \beta_2\left(1 - u_2\right) + \mu\right\}}. \tag{2.3}$$

In the model system described by equation (2.2), we define the control set U as:

$$U = \{(u_1(t), u_2(t)) : 0 \leq u_1 < 1, 0 \leq u_2 < 1, 0 \leq t \leq T\}.$$

The objective is to minimize the function:

$$J = \int_0^T \left(D_1 I_{nf}(t) + \frac{1}{2} w_1 u_1^2 + \frac{1}{2} w_2 u_2^2\right) dt, \tag{2.4}$$

where D_1, w_1, w_2 are positive constants. The terms $\frac{1}{2}w_1u_1^2$ and $\frac{1}{2}w_2u_2^2$ represent the costs associated with controls u_1 and u_2. To minimize infections, we seek optimal controls (u_1^*, u_2^*) such that:

$$J(u_1^*, u_2^*) = \min\{J(u_1, u_2)|(u_1, u_2) \in U\}.$$

The Hamiltonian H is defined as:

$$H(S, E, I_{so}, I_{nf}, R, u_1, u_2, X) = L + X_1 S' + X_2 E' + X_3 I_{so}^{'} + X_4 I_{nf}^{'} + X_5 R'.$$

The specific form of the Hamiltonian is given by:

$$\begin{aligned} H = {} & D_1 I_{nf}(t) + \frac{1}{2} w_1 u_1^2 + \frac{1}{2} w_2 u_2^2 + X_1 \left(\alpha + \gamma_1 I_{so} + \varphi R - \rho S E - \mu S\right) \\ & + X_2 \left(\rho S E - \beta_1 E - \beta_2 E(1-u_2) - \mu E\right) \\ & + X_3 \left(\beta_1 E - \gamma_1 I_{so} - \gamma_2 I_{so}(1-u_1) - \mu I_{so}\right) \\ & + X_4 \left(\beta_2 E(1-u_2) + \gamma_2 I_{so}(1-u_1) - r I_{nf}(1+u_1) - (\mu + \delta_0) I_{nf}\right) \\ & + X_5 \left(r I_{nf}(1+u_1) - \varphi R - \mu R\right). \end{aligned} \tag{2.5}$$

Here, the objective Function J represents the total cost associated with infection levels and control measures. The Hamiltonian H combines the costs of infections and control efforts with the dynamics of the population states, and costate variables X_1, X_2, X_3, X_4, X_5 reflect the marginal value of each state variable

- X_1: Value of susceptible individuals S.
- X_2: Value of exposed individuals E.
- X_3: Value of isolated individuals I_{so}.
- X_4: Value of infected individuals I_{nf}.
- X_5: Value of recovered individuals R.

Lemma 1. *Assuming the set $\{u_1, u_2\}$ minimizes J, we then have adjoint variables $X_1, X_2, \ldots, X_5$ that satisfy the adjoint equations*

$$-\frac{\partial X_i}{\partial t} = \frac{\partial H}{\partial i} \quad \text{with } X_i(t_f) = 0, \quad \text{where } i = S, E, I_{so}, I_{nf}, R.$$

Therefore,

$$\begin{cases} \frac{\partial X_1}{\partial t} & = X_1(\rho E + \mu) - X_2 \rho E, \\ \frac{\partial X_2}{\partial t} & = (X_1 - X_2)\rho S + X_2(\beta_1 + \beta_2(1-u_2) + \mu) - X_3\beta_1 - X_4\beta_2, \\ \frac{\partial X_3}{\partial t} & = (X_3 - X_1)\gamma_1 + (X_3 - X_4)(1-u_1)\gamma_2 + X_3\mu, \\ \frac{\partial X_4}{\partial t} & = (X_4 - X_5)(1+u_1)r + X_4(\mu + \delta_0) - A_1, \\ \frac{\partial X_5}{\partial t} & = (X_5 - X_1)\varphi + X_5\mu. \end{cases} \tag{2.6}$$

The characterized control sets are:

$$u_1^* = \max\{0, \min(1, u_1)\},$$

$$u_2^* = \max\{0, \min(1, u_2)\},$$

where,

$$u_1 = \frac{(X_4 - X_3)\gamma_2 I_{so} + r I_{nf}(X_4 - X_5)}{W_1},$$

$$u_2 = \frac{(X_4 - X_2)\beta_2 E}{W_2}.$$

Proof. Consider $U^* = (u_1^*, u_2^*)$ and $S^*, E^*, I_{nf}^*, I_{so}^*, R$ being the associated solutions. Pontryagin's maximum principle [4, 5, 12] is applied such that there exist

adjoint all variables (2.6) satisfying

$$-\frac{\partial X_1}{\partial t} = \frac{\partial H}{\partial S}, -\frac{\partial X_2}{\partial t} = \frac{\partial H}{\partial E}, -\frac{\partial X_3}{\partial t} = \frac{\partial H}{\partial I_{so}}, -\frac{\partial X_4}{\partial t} = \frac{\partial H}{\partial I_{nf}}, -\frac{\partial X_5}{\partial t} = \frac{\partial H}{\partial R},$$

with transversality conditions $X_1(t_f) = X_2(t_f) = X_3(t_f) = X_4(t_f) = X_5(t_f) = 0$. Within the interior of the set, where $0 < u_i < 1 \; \forall \; i = 1, 2$. We determine the time variant control functions u_1, u_2 when $\dfrac{\partial H}{\partial u_1} = \dfrac{\partial H}{\partial u_2} = 0$. Applying these using (2.5) we get optimal control

$$u_1 = \frac{(X_4 - X_3)\gamma_2 I_{so} + rI_{nf}(X_4 - X_5)}{W_1},$$
$$u_2 = \frac{(X_4 - X_2)\beta_2 E}{W_2}.$$

Hence,

$$u_1^* = \max\left\{0, \min\left(1, \frac{(X_4 - X_3)\gamma_2 I_{so} + rI_{nf}(X_4 - X_5)}{W_1}\right)\right\},$$
$$u_2^* = \max\left\{0, \min\left(1, \frac{(X_4 - X_2)\beta_2 E}{W_2}\right)\right\}.$$

Hence completes the proof. □

Remark 1. *The qualitative analysis of the model (2.2) is presented in Appendix A, which includes a detailed examination of the disease-free equilibrium, endemic equilibrium, and basic reproduction number. Additionally, the results of the parameter estimation and the sensitivity analysis are provided in Appendix A.1 and A.2, respectively.*

3. Effects of Parameters on the Basic Reproduction Number

In this section, we investigate the impacts of isolation rate β_1, infection rate β_2, natural death rate μ, and control variable u_2 on basic reproduction number R_B which is calculated in (A.4), moreover these parameters are directly related in R_B. The values for all parameters are obtained from Table 1. Note that this section is similar to [4]. Here, we consider birth rate $\alpha = 0.25$ and natural death rate $\mu = 0.075$.

3.1. Impact of Isolation and Infection Rate.

The aim of this section is to show the impact of isolation rate β_1 and infection rate β_2 on basic reproduction number R_B. Figure 2, illustrates how the basic reproduction number changes when isolation and infection rate varies.

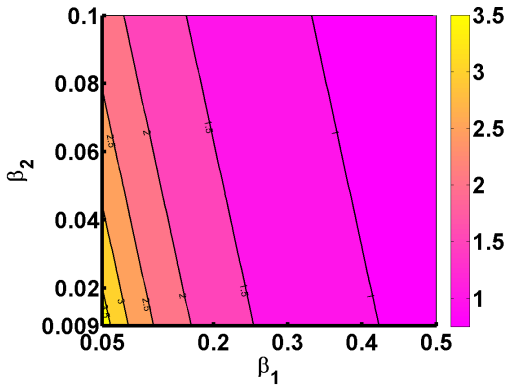

FIGURE 2. Contour plot of β_1, β_2 as a function of R_B.

Figure 2 displays a phase diagram that depicts the relationship between the model parameters: the isolation rate β_1 and the infection rate β_2. The horizontal axis denotes β_1, while the vertical axis indicates β_2. The colored regions reflect the basic reproduction number R_B, an important epidemiological metric that indicates the potential for disease transmission. This 2D plot visually represents how R_B changes in response to the variations in the two model parameters, β_1 and β_2.

3.2. **Impact of Isolation, Infection, and Natural Death Rate.**

This section delineates the impact of isolation rate β_1, infection rate β_2, and natural death rate μ on basic reproduction number R_B. Figure 3, illustrates β_1 vs μ and β_2 vs μ on R_B.

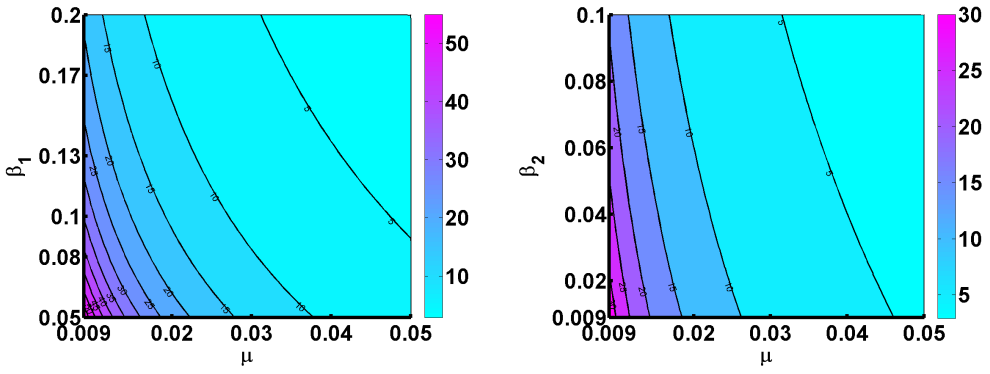

(A) (B)

FIGURE 3. Contour plot of (a) μ, β_1, (b) μ, β_2 as a function of R_B.

Figure 3(a) is a phase diagram showing the relationship between the model parameters β_1 and μ, which are the isolation and natural mortality rates, respectively. The different colored regions in the phase diagram correspond to different values of the basic reproduction number R_B. Figure 3(b) visualizes the relationship between the model parameters β_2, μ, and the basic reproduction number R_B. The figures help to understand how the model parameters, particularly β_1, μ and β_2, μ, influence the basic reproduction number. This information can be used to explore intervention strategies, such as reducing the infection rates through various control measures, to bring the R_B value below 1 and effectively contain the disease outbreak.

3.3. **Impact of Isolation, Infection Rate and Control Variable.**

The purpose of this section is to illustrate the impact of isolation rate β_1, infection rate β_2, and control variable (medical treatment) u_2 on basic reproduction number R_B. Figure 4, visualize β_1 vs u_2 and β_2 vs u_2 on R_B.

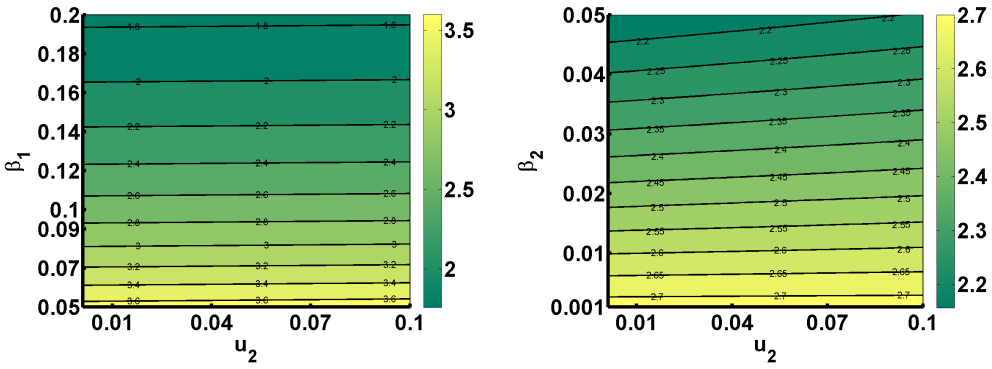

(A) (B)

FIGURE 4. Contour plot of (a) u_2, β_1, (b) u_2, β_2 as a function of R_B.

Figure 4(a) represents the basic reproduction number (R_B) of the disease model (2.2). The x-axis shows the control variable u_2, representing the control measures applied to the exposed class. The y-axis shows the parameter β_1, which is one of the transmission rates in the model. The different colored lines in the figure represent the values of R_B as a function of u_2 and β_1. Similarly, Figure 4(b) illustrates the basic reproduction number where x-axis represents u_2 and y-axis represents infection rate β_2. From the figure, we can conclude that the figure is a visualization of how the basic reproduction number changes as the control measure u_2 and the isolation rate β_1 are varied. This type of plot can aid in understanding how various control strategies influence disease dynamics and highlight the parameter regions where the disease is more likely to be contained or eradicated.

3.4. **Impact of Isolation, Infection, and Recovered Rate.**

In this section, we investigate the impacts of isolation rate β_1, infection rate β_2, and recovered rate r on basic reproduction number R_B. Figure 5, visualizes β_1 vs r and β_2 vs r on R_B.

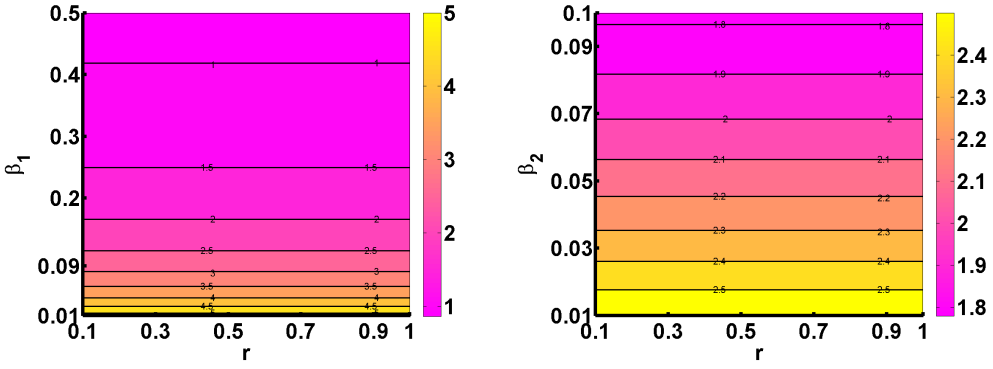

(A) (B)

FIGURE 5. Contour plot of β_1, r and β_2 as a function of R_B.

Figure 5(a) shows a contour plot of the basic reproduction number R_B, as a function where x-axis represents the recovered rate r and y-axis represents the isolation rate β_1.The contour plot shows how R_B changes across various combinations of r and β_1, offering valuable insights into disease dynamics and possible control strategies. Similarly, Figure 5(b) presents a contour plot of the basic reproduction number R_B, where the x-axis indicates the recovery rate r and the y-axis represents the infection rate β_2.

3.5. **Impact of Isolation, Infection Rate and Control Parameter.**

This section illustrate the impact of isolation rate β_1, infection rate β_2, and control parameter u_1 on basic reproduction number R_B. Figure 6, delineates β_1 vs u_1 and β_2 vs u_1 on R_B.

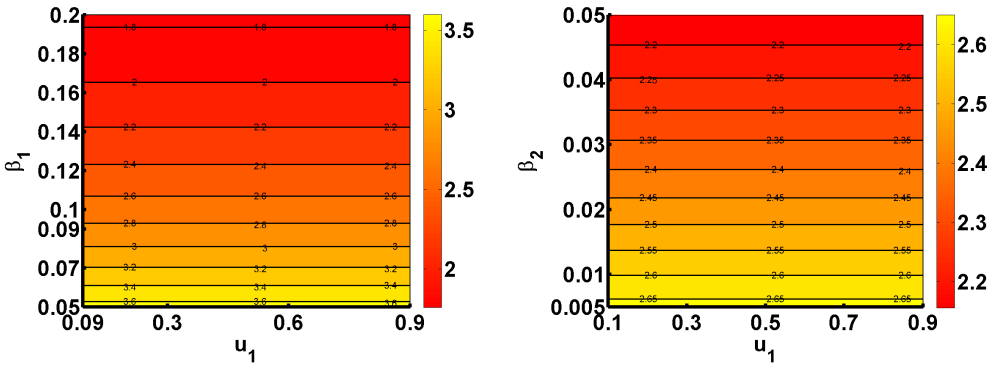

(A) (B)

FIGURE 6. Contour plot of (a) u_1, β_1, (b) u_1, β_2 as a function of R_B.

Figure 6(a) shows how R_B changes as the control parameter u_1 and isolation rate β_1 are varied. By analyzing this figure, one can identify the regions where R_B is less than 1 (indicating disease extinction) and the regions where R_B is greater than 1 (indicating disease persistence). Analogously, Figure 6(b) delineates R_B with respect to β_2 and u_1. This type of visualization is useful for assessing the effectiveness of various control strategies and their influence on disease dynamics, which is essential for developing and implementing effective interventions. Additional computational results for long-term nature are observed and the results are displayed in Appendix B.

4. Optimal Control Strategies

The following figures illustrate the model forecasting of (2.2) using birth rate $\alpha = 0.25$, and natural death rate $\mu = 0.075$ and all the values from Table 1. Here, four cases may arise, namely-

- control parameter u_1 and control variable u_2 persist.
- control parameter u_1 extinct and control variable u_2 persist.
- control parameter u_1 persists and control variable u_2 is extinct.
- control parameter u_1 and control variable u_2 are both extinct.

4.1. **Strategy 1: Existence of Control Parameter and Control Variable.**

The aim of this strategy is to control the parameters (prevention) u_1 and the control variable (medical treatment) u_2, both of which are effective. Figure 7 visualize the scenario of exposed, isolated, infected, and recovered class when $u_1 \neq u_2 \neq 0$.

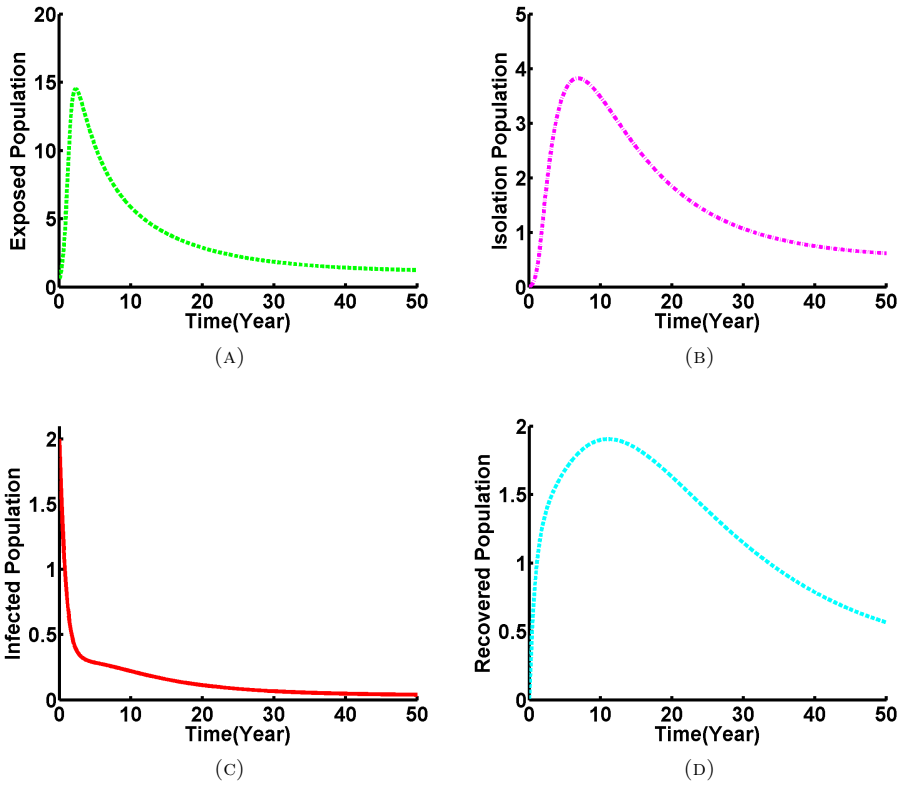

(A) (B) (C) (D)

FIGURE 7. Model prediction of (2.2), where in (a) exposed cases, (b) isolation cases, (c) infected cases, (d) recovered cases.

Figure 7 illustrates the scenario where both control parameter u_1 and control variable u_2 are in effect. In this case, the number of infected and exposed cases shows a gradual decline.

4.2. **Strategy 2: Extinction of Control parameter and Existence of Control Variable.**

The objective of this strategy is without prevention (personal protectiveness) u_1 but with the assistance of medical treatment u_2, it is difficult to prevent the disease which is highlighted in Figure 8.

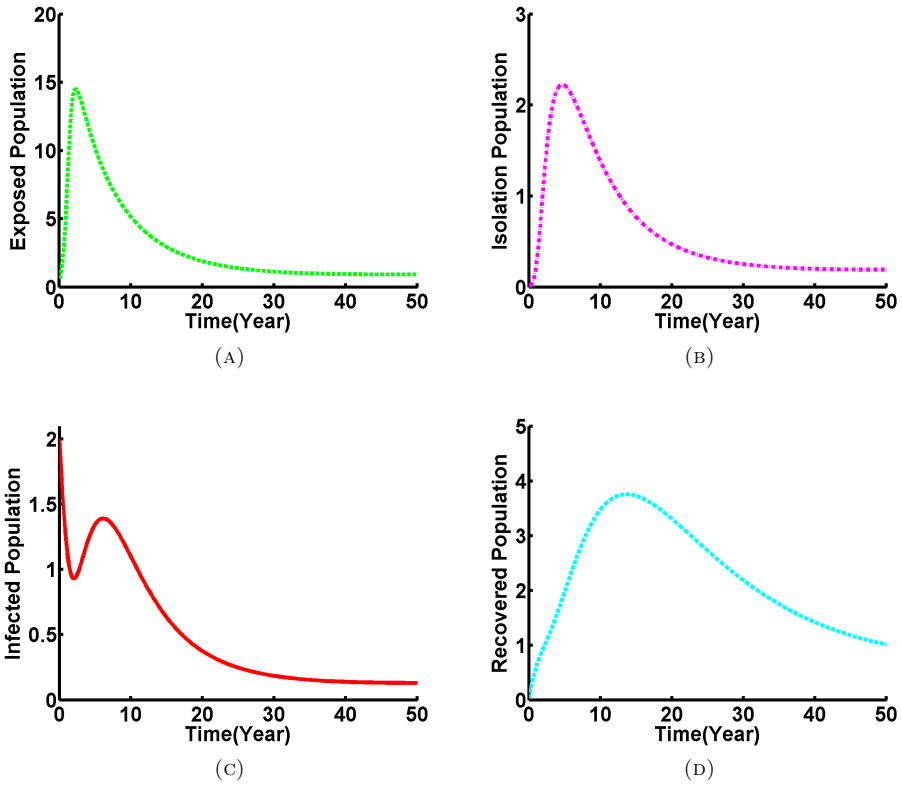

(A) (B) (C) (D)

FIGURE 8. Model prediction of (2.2), where in (a) exposed cases, (b) isolation cases, (c) infected cases, (d) recovered cases.

Figure 8 represents when control parameter $u_1 = 0$ and control variable $u_2 = 0.001$. Here, the number of infected cases increases between almost one year to eight years. After around eight years it will be decreasing and never be increasing again. Note that if $u_2 = 0.01$ or $u_2 = 0.1$, the similar results are obtained. This means that the control variable does not have major impact on the disease when the control parameter $u_1 = 0$.

4.3. **Strategy 3: Persistence of Control parameter and Extinction of Control Variable.**

The goal of this strategy is with prevention (personal protectiveness) u_1 and without medical treatment, the disease can die out which is illustrated in Figure 9.

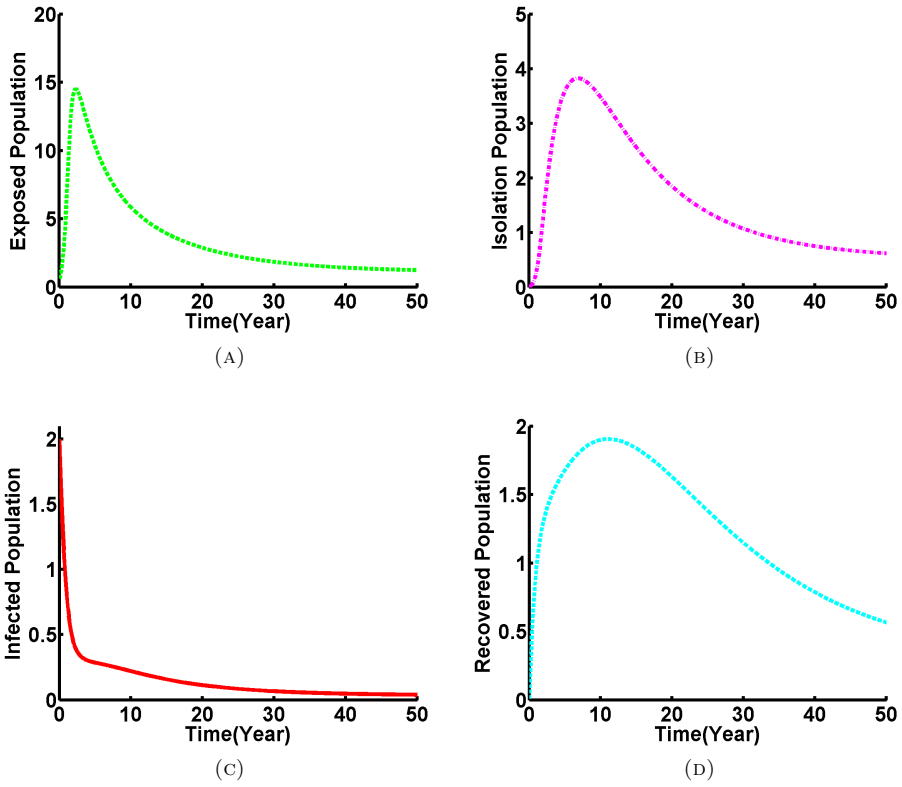

(A) (B) (C) (D)

FIGURE 9. Model prediction of (2.2), where in (a) exposed cases, (b) isolation cases, (c) infected cases, (d) recovered cases.

Figure 9 represents when control parameter $u_1 = 0.9$ and control variable $u_2 = 0$. Here, the number of infected and exposed cases is gradually decreasing.

The next section, 4.4, explores the scenario where both the control parameter and the control variable become extinct. Mathematically, this is referred to as the trivial case.

4.4. **Extinction of Control Parameter and Control Variable.**

The target of this strategy is without prevention u_1 and medical treatment u_2, the disease extinction is difficult which is delineated in Figure 10.

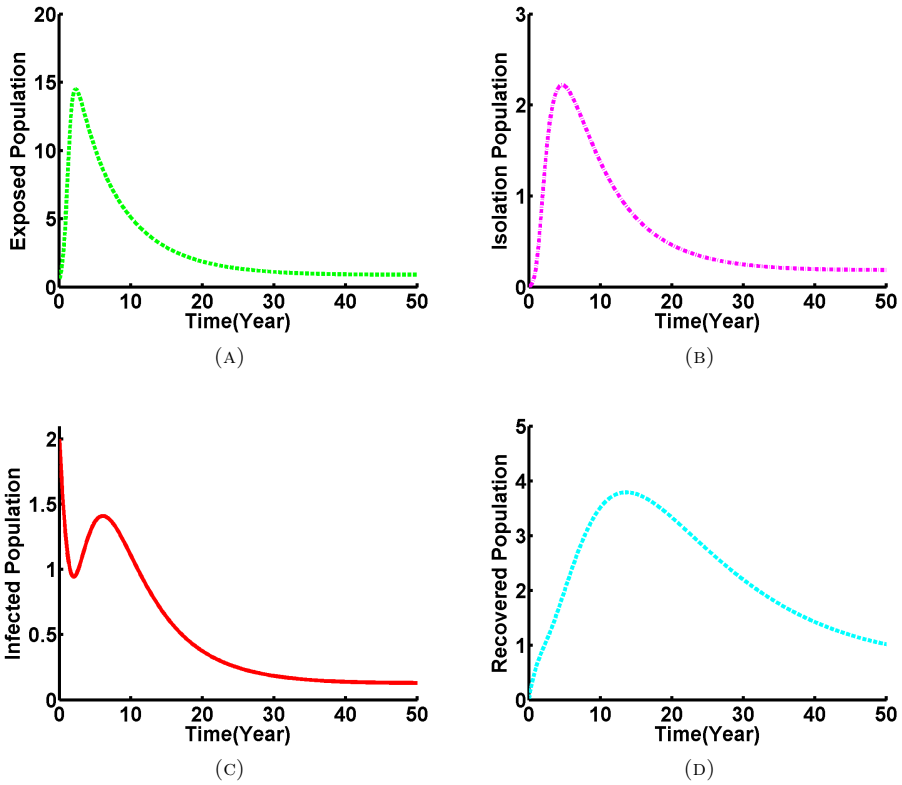

(A) (B) (C) (D)

FIGURE 10. Model prediction of (2.2), where in (a) exposed cases, (b) isolation cases, (c) infected cases, (d) recovered cases.

Figure 10 represents when $u_1 = u_2 = 0$. Here, the number of infected cases rises steadily over a period of approximately one to eight years. After around eight years, the cases begin to decline and do not increase again, consistent with the observations in subsection 4.2.

Remark 2. *From Figures 7, 8, 9 and 10, we can conclude that control parameter u_1 plays a vital role for disease control in this model (2.2) but control variable u_2 does not play significant impact to control the disease.*

4.5. **Combined Strategies.**

This section illustrates the combine strategies which is explained above. Figure 11 delineates the all strategies which can help to understand the translucent scenario of the disease dynamics.

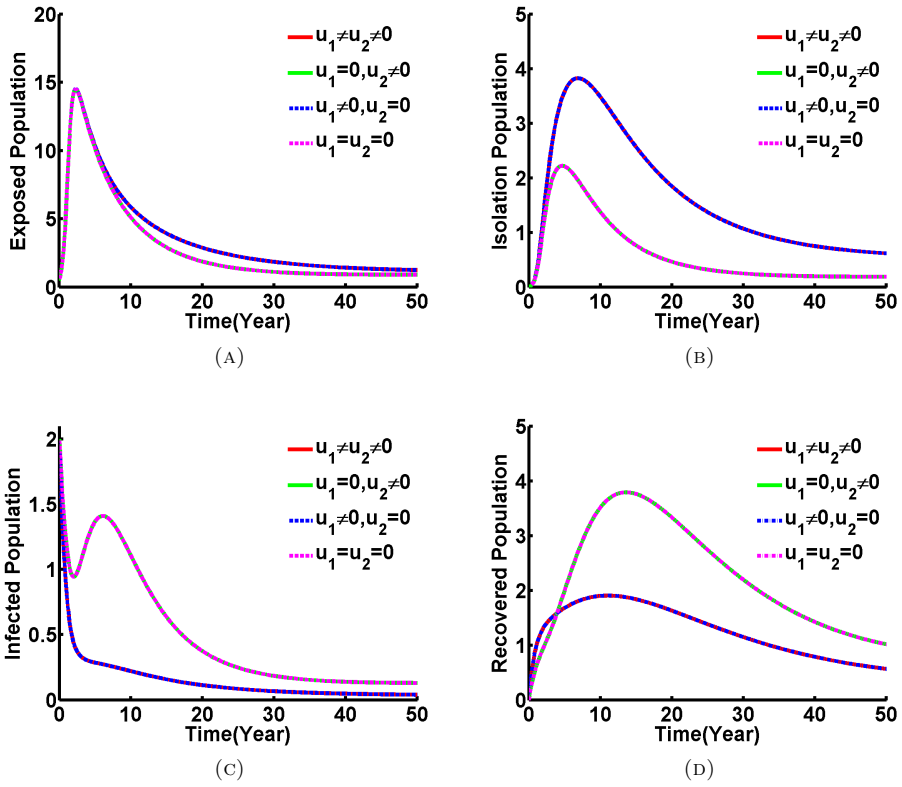

(A) (B) (C) (D)

FIGURE 11. Combined strategies of (2.2), where in (a) exposed cases, (b) isolation cases, (c) infected cases, (d) recovered cases.

Figure 11 illustrates the intricate dynamics of the modeled population and the potential effects of various control strategies on the progression of the epidemic.

4.6. **Effect of Various Values of Control Parameter.**

Example 1.

This experiment for various control parameters u_1 *whenever control variable* u_2 *is fixed. In this example, we consider the fixed value of* $u_2 = 0.001$. *Here, birth rate* $\alpha = 0.25$ *and natural death rate* $\mu = 0.075$ *and all other parameter values are taken from Table 1. Similar study found on* [25].

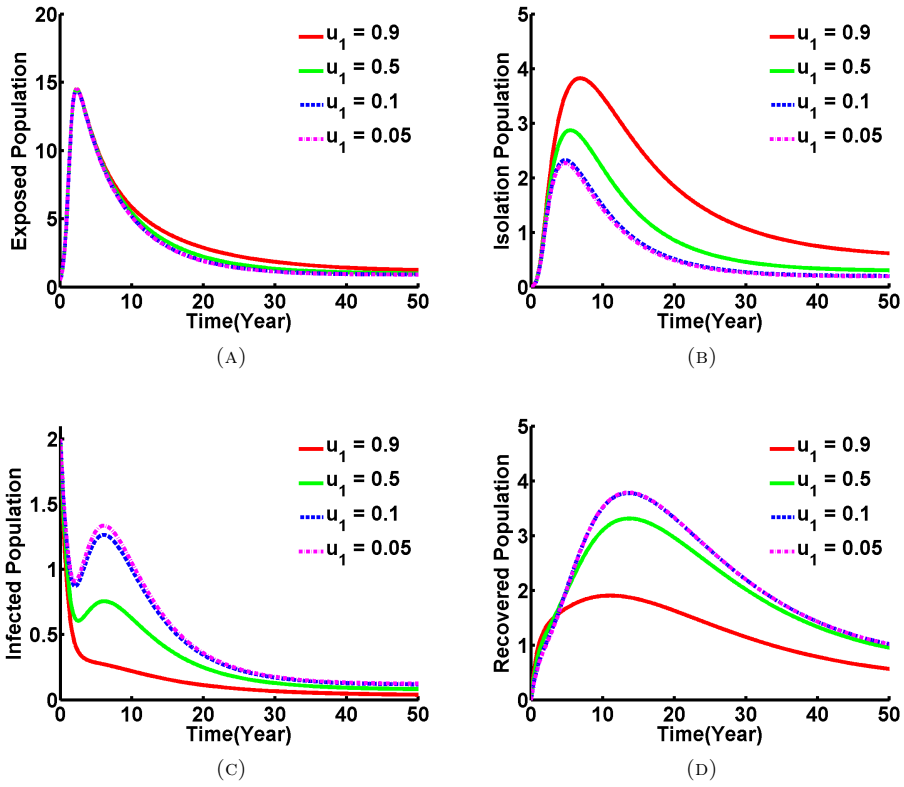

FIGURE 12. Model forecasting of (2.2), where in (a) exposed cases, (b) isolation cases, (c) infected cases, (d) recovered cases.

From Figure 12, it concludes that when the value of control parameter u_1 gradually increases, the disease becomes under control.

This figure shows the model (2.2) forecasting of the epidemic dynamics based on the system of differential equations. The different panels represent the changes in various population groups over time, with the x-axis denoting the time in years and the y-axis representing the population size.

- *(a) Exposed Cases: This panel shows the dynamics of the exposed population. As u_1 increases, the peak of the exposed population decreases and occurs earlier, suggesting that the control measures help to limit the spread of the infection.*
- *(b) Isolated Cases: This panel illustrates the dynamics of the isolated or quarantined population. Higher values of u_1 lead to a more pronounced peak in the isolated population, as more infected individuals are identified and isolated.*

(c) *Infected Cases: This panel depicts the dynamics of the actively infected population. Increasing the control parameter u_1 results in a lower peak and earlier decline in the infected population, indicating the positive impact of the control measures.*

(d) *Recovered Cases: This panel shows the dynamics of the recovered population. As u_1 increases, the peak of the recovered population becomes higher and occurs earlier, reflecting the successful recovery of a larger portion of the population under stricter control measures.*

Figure 12, provides a clear visualization of how the epidemic dynamics are influenced by the control parameter u_1, which represents the effectiveness of the isolation or quarantine measures. By adjusting the value of u_1, policymakers and public health authorities can explore different scenarios and evaluate the potential impacts of various intervention strategies on the progression of the epidemic.

Example 2. *From Example 1, we observe that for the control parameter u_1 the isolation class, infected class, and recovered class significantly change from 0.4 to 0.9 of u_1 in the first 20 years. For this reason, this experiment delineates the impact of the disease for the model (2.2) for the first 20 years when the values of control parameter u_1 are between $0.4 - 0.9$. All other variable and parameter values are sourced from Table 1, with the exception of the values for α and μ. For this example, we consider birth rate $\alpha = 0.25$ and natural death rate $\mu = 0.075$.*

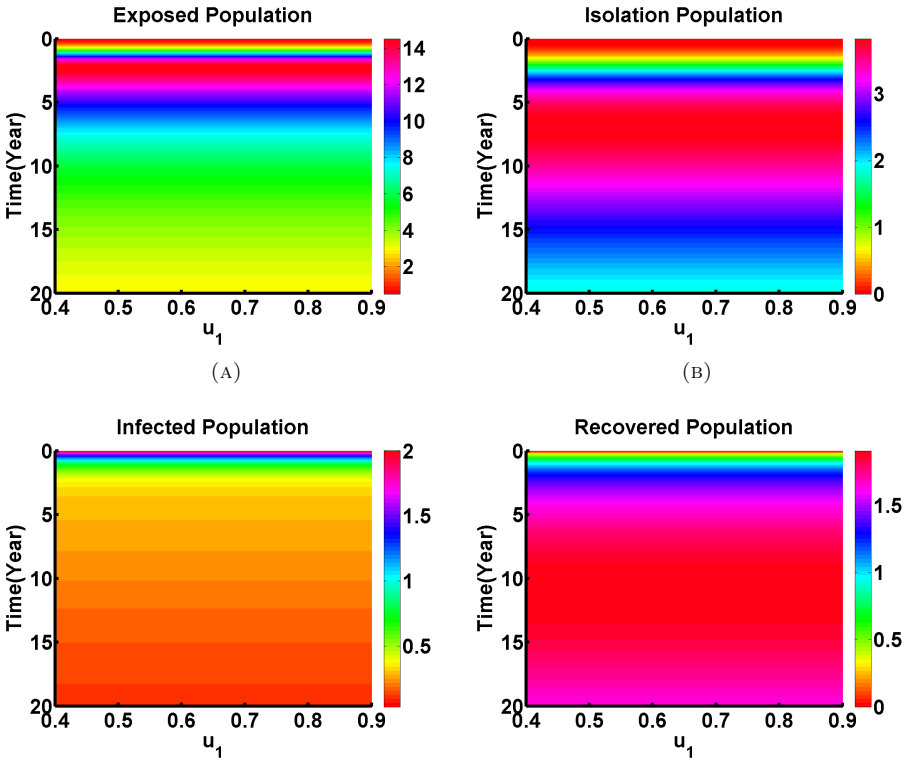

(A) (B) (C) (D)

FIGURE 13. Colormap of the model solution (2.2), where in (a) exposed cases, (b) isolation cases, (c) infected cases, (d) recovered cases.

Figure 13 represents the impact of the control parameter u_1 *from the values of* 0.4 *to* 0.9 *for the first* 20 *years. The following impact is illustrated in Figure 13.*

- *Figure 13(a) illustrates the exposed class which is initially a* 0.5 *million population and it is increasing but after a very short time after almost* 2 *years, it becomes reduced to time.*
- *Figure 13(b) delineates the isolation class which was initially zero and then increasing, after almost* 12 *years it becomes decreasing.*
- *Figure 13(c) represents the infected class which is initially very low then after a very short time within a year it becomes almost* 2 *million but within a short period in that year, it starts reducing to time.*
- *Figure 13(d) illustrates the recovered class which is initially zero then a very short period it is increasing. Almost* 8 *to* 12 *years it becomes increasing significantly and reaches almost* 2 *million which is the highest number*

among the population in the recovered class, then after around 12 *years it becomes reduced to time.*

5. Cost-Effectiveness Analysis

To identify the optimal approach to putting the best control in place to lower MVD in the community, we conducted a cost-effectiveness analysis in this section. We use the incremental cost-effectiveness ratio (ICER) to measure the variations in the expenses and health results of these three strategies. ICER is utilized to evaluate two intervention options, i and j, for mitigating disease transmission, helping to prevent the inefficient use of limited resources. The ICER formula is given below [4, 27].

$$\text{ICER} = \frac{\text{Difference in costs between strategies } i \text{ and } j}{\text{Difference in the number of infections averted between strategies } i \text{ and } j},$$

$(i, j \in \{1, 2, 3\})$. The total number of averted infections is calculated as the difference between the overall number of infected individuals without any controls and those with controls. Meanwhile, the objective function (2.4) in Appendix is utilized to evaluate the overall cost associated with each method. To compute the total cost and the number of infections prevented, we refer to the parameter values provided in Table 1, excluding α and μ. We consider $\alpha = 0.25$ and $\mu = 0.075$. Consequently, Table 2 is organized with the total infection averted ratio (IAR) listed in ascending order. To identify the most cost-effective saving strategy, we calculate the ICER based on the total cost and IAR values.

In Table 2, to calculate the total averted infections (TA), we subtract the final values of the state variables from their initial values. This gives us the total number of infections that were averted over the simulation time. The similar study was found on Section 4.4 in [27]. To calculate the total cost (TC), we assume a cost of 0.5 per unit of control for the isolation strategy (u_1) and a cost of 0.7 per unit of control for the medical treatment strategy (u_2). We then sum up the total cost over the simulation time. The time frame analyzed extends up to 100 units (years). This study is comparable to the findings in [4].

To calculate the total cost (TC) associated with the control strategies for MVD, we assume a cost of 0.5 per unit of control for the isolation strategy (u_1) and a cost of 0.7 per unit of control for the medical treatment strategy (u_2). The total cost can be expressed mathematically as:

$$TC = (C_{u_1} \cdot u_1 + C_{u_2} \cdot u_2) \cdot T$$

where $C_{u_1} = 0.5$, $C_{u_2} = 0.7$, u_1 and u_2 are the control efforts, and T is the total simulation time. Summing these costs over the simulation period allows for an assessment of the financial implications of the implemented strategies. These cost assumptions are grounded in empirical research that highlights the economic aspects of public health interventions [28]. The study by [28] discusses the cost-effectiveness of isolation and treatment strategies in controlling infectious diseases, emphasizing that investments in these areas can lead to significant reductions in disease transmission and overall healthcare costs [28].

Approach	Optimal strategies	Total infections averted (TA)	Total cost (TC)
2	u_2^*	2081.667816	0.166115
1	u_1^*, u_2^*	2771.896493	-2.300260
3	u_1^*	2771.911482	-2.526799

TABLE 2. The overall cost of each technique and the number of infections prevented.

Note that the strategy that has the highest ICER values is excluded from the ICER computations at each stage.

- Two competing strategies (2) and (1), where strategy (1) is more effective than strategy (2) (TA(1) > TA(2)), and the ICER values are calculated as follows:

$$\text{ICER}(2) = \frac{\text{TC}(2)}{\text{TA}(2)} = \frac{0.166115}{2081.667816} = 0.000079799,$$

$$\text{ICER}(1) = \frac{\text{TC}(1) - \text{TC}(2)}{\text{TA}(1) - \text{TA}(2)} = \frac{-2.300260 - 0.166115}{2771.896493 - 2081.667816} = -0.0035732723.$$

  The results obtained from the ICER(2) and ICER(1) values show that strategy (1) is cheaper than strategy (2). Hence, strategy (2) is eliminated from the set of alternatives, and then strategies (1) and (3) are compared.

-

$$\text{ICER}(1) = \frac{\text{TC}(1)}{\text{TA}(1)} = \frac{-2.300260}{2771.89643} = -0.0008298506,$$

$$\text{ICER}(3) = \frac{\text{TC}(3) - \text{TC}(1)}{\text{TA}(3) - \text{TA}(1)} = \frac{-2.526799 + 2.300260}{2771.911482 - 2771.896493} = -15.1136833678.$$

  Ultimately, the values of ICER(1) and ICER(3) indicate that strategy (3) is more cost-effective than strategy (1). Therefore, strategy (1) is removed from the list of options.

Thus, we conclude that strategy (3) is the most cost-effective option among all the strategies for controlling MVD interventions.

The ICER values provide crucial insights into the cost-effectiveness of different health interventions. A lower ICER indicates that a strategy offers more health benefits per unit of cost, making it a more favorable option for public health decision-making. In the context of the strategies analyzed, the negative ICER values suggest that certain interventions not only save costs but also provide significant health benefits, which is vital for resource allocation in public health. These results can guide policymakers in selecting the most cost-effective strategy by highlighting options that maximize health outcomes while minimizing expenditures. By comparing the ICER values, decision-makers can prioritize interventions that provide the greatest return on investment, ensuring efficient use of limited healthcare resources. The elimination of less effective strategies ensures that funding is directed toward interventions that yield the best health outcomes. In real-world settings,

thresholds or benchmarks for determining whether a strategy is considered "cost-effective" often vary by country and health system. Commonly cited thresholds range from $50,000 to $100,000 per Quality-Adjusted Life Year (QALY) gained in the United States, while other countries may use lower thresholds based on economic conditions. These benchmarks help establish a standard for evaluating the relative value of healthcare interventions and facilitate informed decision-making in public health policy [29, 30, 31].

6. Result and Discussion

The proposed model demonstrates that effective control of Marburg Virus Disease (MVD) necessitates the isolation of infected individuals, which is critical for preventing transmission. Our findings indicate that achieving a 99% efficacy rate in prevention efforts can significantly mitigate the spread of the virus. The most effective strategy identified combines isolation, personal protective measures, and the enhancement of natural immunity. Simulations underscore the significance of improving the natural immunity of isolated individuals through dietary modifications, hygiene practices, and supplementary medicine. This multifaceted approach is essential for the potential eradication of MVD. Our findings are consistent with existing literature on Ebola and other hemorrhagic fevers, reinforcing the efficacy of isolation as a primary control measure. Previous studies have similarly emphasized the role of isolation in reducing transmission rates. The integration of natural immunity dynamics within our model further enriches the discourse on control strategies, suggesting that individual health practices can effectively complement public health interventions. Furthermore, real-world interventions during past outbreaks have demonstrated that rigorous isolation protocols, combined with community engagement and health education, have successfully contained similar viral infections. By comparing our model with these interventions, we highlight the necessity of a holistic approach that incorporates both individual behavioral changes and systemic healthcare strategies. In conclusion, the prevention of MVD relies on the dual strategies of isolating infected individuals and harnessing natural immunity. Our deterministic mathematical model underscores that a combination of isolation, supportive healthcare, and healthy lifestyle promotion is critical in combating MVD. Prioritizing these strategies is essential for effectively managing and ultimately eliminating this deadly disease.

Acknowledgement. The author M. Kamrujjaman acknowledge the University Grants Commission (UGC), and the University of Dhaka, Bangladesh for supplementary support of this research.

Competing interests

The authors declare no conflict of interest.

Ethical approval

N/A.

Data availability/Data sharing

No human data used in this study.

CRediT authorship contribution statement

Zasmin Haque: Conceptualization, Data curation, Formal analysis, Methodology, Software, Validation, Writing– original draft.
Md. Mashih Ibn Yasin Adan: Data curation, Formal analysis, Methodology, Validation, Software, Writing– original draft, Writing– review & editing.
Md. Kamrujjaman: Conceptualization, Validation, Resources, Investigation, Funding acquisition, Software, Supervision, Writing– review & editing.
All authors have read and agreed to the published version of the manuscript.

Ethics Statement

None.

REFERENCES

[1] "Marburg hemorrhagic fever (marburg hf)," 25 February 2019. Archived from the original on 19 October 2022. Retrieved 16 February 2020. https://www.cdc.gov/marburg/about/index.html.

[2] "Marburg virus disease," in *World Health Organization*. https://www.who.int/news-room/fact-sheets/detail/marburg-virus-disease.

[3] ScienceDirect, "Marburg virus – an overview." https://www.sciencedirect.com/topics/veterinary-science-and-veterinary-medicine/marburg-virus, 2021. Archived on 21 October 2021. Accessed on 12 August 2020.

[4] C. C. W. Fatmawati, A. R. T., A. C., H. F. F., and Tasmi, "A pontryagin's maximum principle and optimal control model with cost-effectiveness analysis of the covid-19 epidemic," *Dec. Anal. Jour.*, vol. 8, p. 100273, 2023. https://www.sciencedirect.com/science/article/pii/S2772662223001133.

[5] L. S. Pontryagin, V. G. Boltyanskii, R. V. Gamkrelidze, and E. F. Mishchenko, *The Mathematical Theory of Optimal Processes*. Wiley, New York, 1962. https://onlinelibrary.wiley.com/doi/abs/10.1002/zamm.19630431023.

[6] M. I. Kamien and N. L. Schwarts, *Dynamic Optimization: the Calculus of Variations and Optimal Control in Economics and Management*. 2nd ed., Elsevier, Science B.V., 1991. https://zuhermanrustam.wordpress.com/wp-content/uploads/2015/02/kamienschwartz911.pdf.

[7] D. Hull, *Optimal Control Theory for Applications*. Springer-Verlag, New York, Berlin, Heidelberg, 2003. https://link.springer.com/book/10.1007/978-1-4757-4180-3.

[8] W. H. Fleming and R. W. Rishel, *Deterministic and Stochastic Optimal Control*. Springer Verlag, New York, 1975. https://link.springer.com/book/10.1007/978-1-4612-6380-7.

[9] S. Ahmed, S. Rahman, and M. Kamrujjaman, "Optimal treatment strategies to control acute hiv infection," *Inf. Dis. Mod.*, vol. 6, pp. 1202–1219, 2021. https://doi.org/10.1016/j.idm.2021.09.004.

[10] D. J. Washachi, H. O. Orapine, A. A. Baidu, and J. A. Amoka, "Mathematical model for the transmission dynamics of marburg virus diseases with contact tracing and effective quarantine," *FUW Trends in Science & Technology Journal*, vol. 7, no. 3, pp. 35 – 43, 2022. https://www.ftstjournal.com/uploads/docs/73%20Article%206%20pp%2035-43.pdf.

[11] Z. Haque, M. Kamrujjaman, M. S. Alam, and M. H. A. Biswas, "Marburg virus and risk factor among infected population: A modeling study," *Malay. Jour. Math. Sci.*, vol. 18, no. 1, p. 141–165, 2024. https://doi.org/10.47836/mjms.18.1.09.

[12] M. A. Hye, M. A. H. Biswas, M. F. Uddin, and M. Saifuddin, "Mathematical modeling of covid-19 and dengue co-infection dynamics in bangladesh: Optimal control and data-driven analysis," *Comp. Math. Mod.*, vol. 33, pp. 173–192, 2023. https://link.springer.com/article/10.1007/s10598-023-09564-7.

[13] M. U. E. Michael, L. O. Omenyi, E. Nwaeze, K. O. Elebute, F. Oyahkire, G. Ozoigbo, and M. Ekahtor, "Asymptotic study of divorce model with pre-marriage preparedness as control," *Malay. Jour. Math. Sci.*, vol. 17, no. 2, p. 113–133, 2023. https://mjms.upm.edu.my/lihatmakalah.php?kod=2023/June/17/2/113-133.

[14] Y. Zhou and Y. Liang, "An optimal strategy for hiv multitherapy," *Jour. Comput. and Appl. Math.*, vol. 263, pp. 326–337, 2014. https://www.sciencedirect.com/science/article/pii/S0377042713006778.

[15] E. L. Wong, C. K. Wong, P. C. Leung, and W. K. C. Lam, "The efficacy of herbal therapy on quality of life in patients with breast cancer: Self-control clinical trial," *Patient Preference and Adherence*, vol. 4, pp. 223–229, 2010. https://doi.org/10.2147/PPA.S10961.

[16] M. H. A. Biswas, "Necessary conditions for optimal control problems with state constraints: Theory and applications", phd thesis," *PhD Thesis, Department of Electrical and Computer Engineering*, 2013. https://repositorio-aberto.up.pt/bitstream/10216/69742/2/27545.pdf.

[17] J. M. Orellana, "Optimal control for hiv multitherapy enhancement," *C. R. Math.*, vol. 348, pp. hal–00423481f, 2009. https://hal.science/hal-00423481/document.

[18] M. H. A. Biswas, M. M. Haque, and U. K. Mallick, "Optimal control strategy for the immunotherapeutic treatment of hiv infection with state constraint," *Opt. Con. Appl. Meth.*, vol. 40, no. 4, pp. 807–818, 2019. https://onlinelibrary.wiley.com/doi/10.1002/oca.2516.

[19] U. E. Michael, L. O. Omenyi, K. O. Elebute, and A. A. Offia, "Local and global stability analysis of a covid-19 model dynamics with healthy diet as control," *J. Math. Comput. Sci.*, vol. 12, 2022. https://scik.org/index.php/jmcs/article/view/7462.

[20] M. H. A. Biswas, L. T. Paiva, and M. D. Pinho, "A seir model for control of infectious diseases with constraints," *Math. Biosci. Eng.*, vol. 11, no. 4, p. 761–784, 2014. http://dx.doi.org/10.3934/mbe.2014.11.761.

[21] K. Dhama, K. Karthik, and R. Khandia, "Medicinal and therapeutic potential of herbs and plant metabolites/extracts countering viral pathogens - current knowledge and future prospects," *Current Drug Metabolism*, vol. 19, no. 3, pp. 236–263, 2018. https://doi.org/10.2174/1389200219666180129145252.

[22] R. M. Neilan and S. Lenhart, "An introduction to optimal control with an application in disease modeling," *DIMACS Ser. Dis. Math.*, vol. 75, p. 67–81, 2010. https://doi.org/10.1090/dimacs/075/03.

[23] K. N. Islam, T. Parvin, and M. H. A. Biswas, "Dynamic optimization applied to a criminological model for reducing the spread of societal corruption," *Khulna University Studies*, 2022. https://doi.org/10.53808/KUS.2022.ICSTEM4IR.0148-se.

[24] R. I. Gweryina, M. Y. Kura, and E. Okwu, "An epidemiological model of corruption with immunity clause in nigeria," *Worl. Jour. Mod. and Sim.*, vol. 15, no. 3, p. 262–275, 2019. https://www.wjms.org.uk/journal/1746-7233WJMS/wjmsvol15no04paper02.pdf.

[25] M. S. Mahmud, M. Kamrujjaman, and M. M. I. Y. Adan, "Vaccine efficacy and sars-cov-2 control in california and u.s. during the session 2020-2026: A modeling study," *Inf. Dis. Mod.*, vol. 7, no. 1, pp. 62–81, 2022. https://doi.org/10.1016/j.idm.2021.11.002.

[26] C. J. Silva and D. F. M. Torres, "Optimal control for a tuberculosis model with reinfection and post-exposure interventions," *Math. Bio.*, vol. 244, no. 2, p. 154–164, 2013. https://doi.org/10.1016/j.mbs.2013.05.005.

[27] A. Kouidere, O. Balatif, and M. Rachik, "Cost-effectiveness of a mathematical modeling with optimal control approach of spread of covid-19 pandemic: A case study in peru," *Chao., Sol. & Frac.: X*, vol. 10, p. 100090, 2023. https://doi.org/10.1016/j.csfx.2022.100090.

[28] U. Suthutvoravut, P. Kunakorntham, and A. Semayai, "Cost-effectiveness analysis of isolation strategies for asymptomatic and mild symptom covid-19 patients," *Cost Eff. Resour. Alloc.*, vol. 21, no. 85, pp. 1–9, 2023. https://doi.org/10.1186/s12962-023-00497-x.

[29] D. D. Kim and A. Basu, "How does cost-effectiveness analysis inform health care decisions?," *AMA J. Ethics.*, vol. 23, no. 8, pp. 639–647, 2021. 10.1001/amajethics.2021.639.

[30] "Cost-effectiveness, the qaly, and the evlyg," *Institute for Clinical and Economic Review.* https://icer.org/our-approach/methods-process/cost-effectiveness-the-qaly-and-the-evlyg/.

[31] "Cost-effectiveness analysis," in *U.S. Department of Veterans Affairs*, Accessed 12 April, 2024. https://www.herc.research.va.gov/include/page.asp?id=cost-effectiveness-analysis.

[32] "Marburg virus disease)," Accessed 01 May, 2024. https://www.cdc.gov/marburg/about/index.html.

[33] N. Chitnis, J. M. Hyman, and J. M. Cushing, "Determining important parameters in the spread of malaria through the sensitivity analysis of a mathematical model," *Bull. Math. Biol.*, vol. 70, p. 1272–1296, 2008. https://doi.org/10.1007/s11538-008-9299-0.

[34] M. A. Omoloye and S. O. Adewale, "Mathematical analysis of sensitive parameters on the dynamical transmission of ebola-malaria coinfections," *Int. Jour. Com. Sci. and Inf. Sec.*, vol. 19, no. 7, p. 21–45, 2021. https://doi.org/10.1155/2022/5445281.

Appendix

Appendix A. Qualitative Analysis

First here we explain the boundedness and positivity of the model (2.2). The region $\Omega = \left\{(S, E, I_{so}, I_{nf}, R) \in R_+^5 : N_H(t) \leq \frac{\alpha}{\mu}\right\}$ is positive invariant set. From the total population size over a time t, then

$$\frac{dN_H}{dt} = \alpha - \mu N_H - \delta_0 I_{nf}. \tag{A.1}$$

Since $N_H(t)$ is considered to remain constant over time t, we have $\frac{dN_H}{dt} = 0$. If the disease-induced death rate (δ_0) is zero, then equation (A.1) simplifies to $N_H(t) \leq \frac{\alpha}{\mu}$ for $t \geq 0$. Consequently, Ω is a positively invariant set, and within this set, the model (2.2) is both epidemiologically and mathematically well-defined.

Let $D_{fe}^p\left(S^{Df}, E^{Df}, I_{so}^{Df}, I_{nf}^{Df}, R^{Df}\right)$ represent the disease-free equilibrium point (DFE) of the model (2.2). To find DEF we have,

$$\frac{dS^{Df}}{dt} = \frac{dE^{Df}}{dt} = \frac{dI_{so}^{Df}}{dt} = \frac{dI_{nf}^{Df}}{dt} = \frac{dR^{Df}}{dt} = 0. \tag{A.2}$$

Since, infection is not found at DFE then $I_{so}^{Df} = I_{nf}^{Df} = R^{Df} = 0$; i.e. $E^{Df} = 0$ and $S^{Df} = \frac{\alpha}{\mu}$. Therefore, the disease-free equilibrium point is given by $D_{fe}^p\left(\frac{\alpha}{\mu}, 0, 0, 0, 0\right)$. Let $E_{Ep}\left(S^{Ep}, E^{Ep}, I_{so}^{Ep}, I_{nf}^{Ep}, R^{Ep}\right)$ denote the endemic equilibrium point (EEP) of the model (2.2). To find EEP we have,

$$\frac{dS^{Ep}}{dt} = \frac{dE^{Ep}}{dt} = \frac{dI_{so}^{Ep}}{dt} = \frac{dI_{nf}^{Ep}}{dt} = \frac{dR^{Ep}}{dt} = 0. \tag{A.3}$$

Solving the model (2.2) using the above equation (A.3) we get

$$S^{Ep} = \frac{A_1}{\rho},\ E^{Ep} = \frac{\mu A_1 A_2 A_3 A_4 - \alpha\rho A_2 A_3 A_4}{\rho[\gamma_1\beta_1 A_3 A_4 + \varphi\{A_2\beta_2(1-u_2) + \gamma_2(1-u_1)\beta_1\} - A_1 A_2 A_3 A_4]},$$
$$I_{so}^{Ep} = \frac{\beta_1 E^{Ep}}{A_2},\ I_{nf}^{Ep} = \frac{A_2\beta_2(1-u_2) + \gamma_2\beta_1(1-u_1)}{A_2 A_3} E^{Ep},$$
$$R^{Ep} = \frac{A_2 A_3 r(1+u_1)[A_2\beta_2(1-u_2) + \gamma_1\beta_1(1-u_1)]}{A_2 A_3 A_4} E^{Ep},$$

where,

$$A_1 = \beta_1 + \beta_2(1-u_2) + \mu,\ \ A_2 = \gamma_1 + \gamma_2(1-u_1) + \mu$$
$$A_3 = r(1+u_1) + (\mu + \delta_0),\ \ A_4 = \varphi + \mu.$$

Also the model (2.2) has a basic reproduction number given by

$$R_B = \frac{\alpha\rho}{\mu\left\{\beta_1 + \beta_2\left(1-u_2\right) + \mu\right\}}. \tag{A.4}$$

Using the parameter values from Table 1, we calculate $R_B = 0.06038$ ($\mathcal{R}_0 = 0.1694$ [11]), indicating that the disease can be effectively controlled through the optimal control measures outlined in the model (2.2).

A.1. **Parameter Estimation Techniques.**

We employ the least-squares method for parameter estimation, using the fmincon function from MATLAB's Optimization Toolbox. The objective of least-squares estimation is to determine parameter values that minimize the following objective function:

$$f(\varnothing, n) = \sum_{j=1}^{n} \left\{ I_1(t) - \widehat{I_1}(t) \right\}^2.$$

Here, $\varnothing$ represents the parameter vector being estimated by this method, n is the number of data points, $I_1(t)$ indicates the actual number of MVD-infected individuals, and $\widehat{I_1}(t)$ denotes the number of infected individuals predicted by the simulation. To estimate the parameters, we align the model with the annual new cases of MVD patients. The calculated parameters are given in Table 1.

To estimate the parameters using the least-squares method, data was collected from various reliable sources, including epidemiological reports from the World Health Organization (WHO) [2] and local health departments [32], which provided documented cases of Marburg Virus Disease (MVD) infections. Additionally, hospital records were analyzed to obtain precise figures on new cases and recovery rates. Field studies conducted in affected regions offered insights into transmission dynamics, while surveys with healthcare professionals provided qualitative data to support quantitative findings. The validation of parameters involved cross-validation, where the dataset was split into training and testing subsets, and sensitivity analyses to assess the impact of parameter variations on model predictions. Historical data comparisons ensured that predicted values aligned with observed trends, and expert reviews were conducted to confirm the estimates against current scientific literature [2, 32].

A.2. **Sensitivity Analysis of R_B.**

In the control model (2.2), we applied the normalized forward sensitivity index [33] for a variable concerning a parameter, using the approach outlined by Omoloye et al. [34] to conduct the sensitivity analysis. This gives the percentage of influence each parameter has no infection transmission and outbreak of this diseases. The sensitivity elasticity indices of R_B can be computed using partial derivative is given by $\aleph_{\alpha}^{R_B} = \frac{\partial R_B}{\partial \epsilon} \cdot \frac{\epsilon}{R_B}$; where ϵ is a parameter present in the reproduction number R_B. Applying sensitivity index, we have

$$\aleph_{\alpha}^{R_B} = \frac{\partial R_B}{\partial \alpha} \cdot \frac{\alpha}{R_B} = 1$$

$$\aleph_{\rho}^{R_B} = \frac{\partial R_B}{\partial \rho} \cdot \frac{\rho}{R_B} = 1$$

$$\aleph_{\beta_1}^{R_B} = \frac{\partial R_B}{\partial \beta_1} \cdot \frac{\beta_1}{R_B} = -0.01710488$$

$$\aleph_{\beta_2}^{R_B} = \frac{\partial R_B}{\partial \beta_2} \cdot \frac{\beta_2}{R_B} = -0.01611330$$
$$\aleph_{u_2}^{R_B} = \frac{\partial R_B}{\partial u_2} \cdot \frac{u_2}{R_B} = -0.96667811.$$

Parameter	Sensitivity Index
α	1
ρ	1
u_2	-0.966678109
β_1	-0.01710488
β_2	-0.0161133

TABLE A1. Sensitivity index related to each model parameter.

The sensitivity analysis presented in Table A1 highlights the influence of key parameters on disease dynamics. The parameters α (the natality rate of susceptible individuals) and ρ (the rate of exposure) exhibit a positive sensitivity index of 1, indicating that increases in these parameters will significantly enhance the spread of the disease. Conversely, the control variable u_2 which represents efforts to seek medical treatment and immunity from recovered individuals has a strong negative sensitivity index of -0.966678109. This suggests that enhancing medical treatment efforts will substantially reduce disease prevalence. Additionally, the parameters β_1 (rate of isolation) and β_2 (infection rate among the exposed population) show negative sensitivity indices, indicating that increases in isolation efforts and reduced infection rates among the exposed can mitigate the disease's spread. Overall, this analysis underscores the model's sensitivity to changes in these critical parameters, emphasizing the importance of targeted interventions in controlling MVD outbreaks.

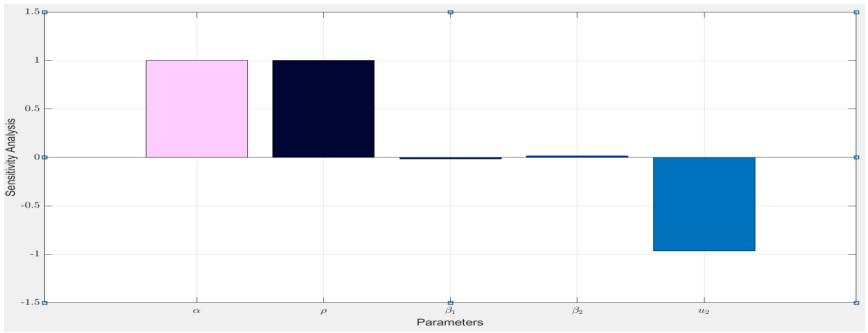

FIGURE 14. The sensitivity of the reproduction number in relation to all parameters.

Appendix B. Long-period Computational Forecasting

In this section, we conducted numerical simulations of the system (2.2) using the ODE45 solver in MATLAB to validate our analytical results. The parameter values utilized in the simulation are presented in Table 1, which includes some estimated, assumed, and best-fit values for the model. The initial conditions are as follows: $S(0) = 20$, $E(0) = 0.5$, $I_{so}(0) = 0$, $I_{nf}(0) = 2$, and $R(0) = 0$. All populations are estimated in millions.

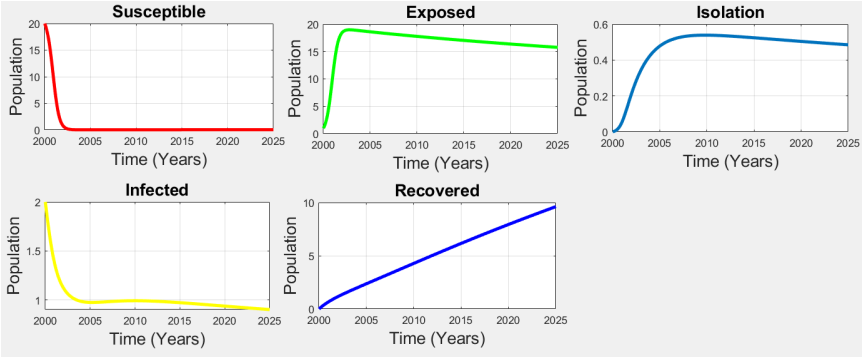

Figure 15. Numerical simulation of MVD infection of the individuals (without control model [11]) with time (25 years).

In the figure above, we notice a rapid rise in the number of isolated individuals, which coincides with a sharp decrease in the number of infected individuals. This suggests that prompt isolation of individuals has a substantial impact on reducing the infection rate.

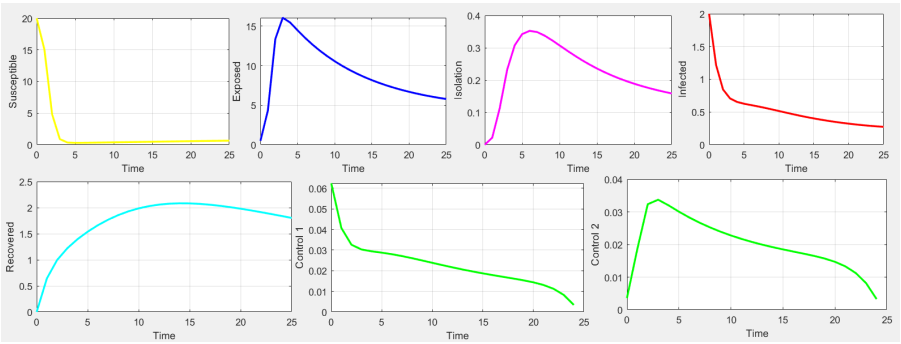

Figure 16. Numerical simulation of MVD infection among individuals (with control model) over a 25-year period.

By comparing the two figures (15 and 16) above, we observe that increasing the number of isolated individuals while implementing control measures in our

model leads to a significant decrease in infections within the overall population. Even as the number of isolated individuals declines over time, the sustained application of control measures continues to result in a steady reduction in infections. This illustrates the effectiveness of these control measures in lowering the infection rate.

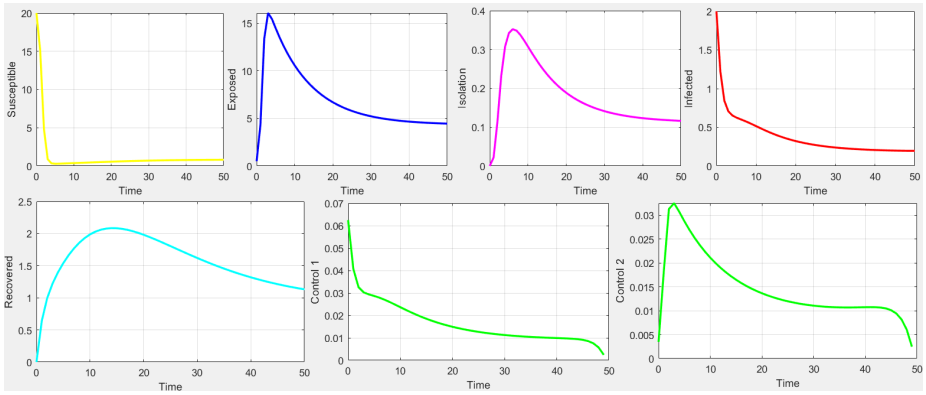

FIGURE 17. Numerical simulation of MVD infection among individuals (with control model) over a 50-year period.

In Figure 17, when we stopped using the control in our model, the infection continued to spread in the population without diminishing. The infection rate never decreased. Meanwhile, even though the isolation rate remained steady, the recovery rate started to decline. This suggests that without ongoing control measures, the situation worsens over time.

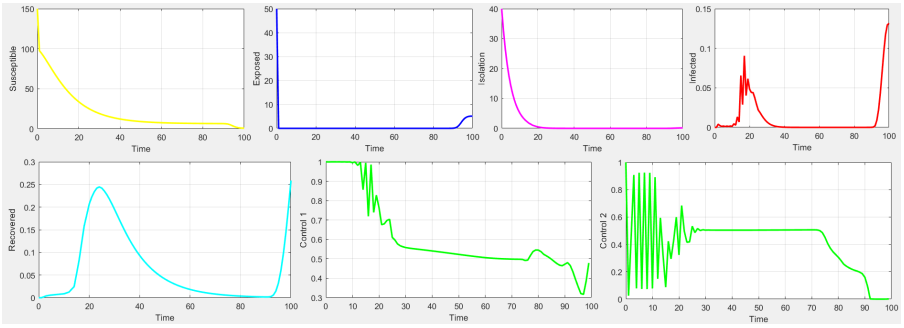

FIGURE 18. Numerical simulation of MVD infection among individuals (with control model) over a 100-year period.

From Figure 18, we noted that at first, when full controls and isolation were implemented, the infection rate exhibited continuous fluctuations. After a period,

the recovery rate increased significantly. However, upon reducing the isolation rate, the infection rate also declined and was nearly eradicated over time with the application of two steady control measures. In contrast, when we lessened the use of controls in our model, the infection rate surged rapidly. This highlights the critical need to maintain control measures for effectively managing the infection rate. The initial fluctuations in the infection rate indicate that control measures require time to stabilize the situation. Over time, consistent application of these controls results in a marked increase in the recovery rate and a decrease in the infection rate.